Study of the Suppressed Decays $B^{\pm} \to [K^{\mp}\pi^{\pm}]_D K^{\pm}$ at Belle

K. Abe,[10] K. Abe,[46] N. Abe,[49] I. Adachi,[10] H. Aihara,[48] M. Akatsu,[24] Y. Asano,[53]
T. Aso,[52] V. Aulchenko,[2] T. Aushev,[14] T. Aziz,[44] S. Bahinipati,[6] A. M. Bakich,[43]
Y. Ban,[36] M. Barbero,[9] A. Bay,[20] I. Bedny,[2] U. Bitenc,[15] I. Bizjak,[15] S. Blyth,[29]
A. Bondar,[2] A. Bozek,[30] M. Bračko,[22, 15] J. Brodzicka,[30] T. E. Browder,[9] M.-C. Chang,[29]
P. Chang,[29] Y. Chao,[29] A. Chen,[26] K.-F. Chen,[29] W. T. Chen,[26] B. G. Cheon,[4]
R. Chistov,[14] S.-K. Choi,[8] Y. Choi,[42] Y. K. Choi,[42] A. Chuvikov,[37] S. Cole,[43]
M. Danilov,[14] M. Dash,[55] L. Y. Dong,[12] R. Dowd,[23] J. Dragic,[23] A. Drutskoy,[6]
S. Eidelman,[2] Y. Enari,[24] D. Epifanov,[2] C. W. Everton,[23] F. Fang,[9] S. Fratina,[15]
H. Fujii,[10] N. Gabyshev,[2] A. Garmash,[37] T. Gershon,[10] A. Go,[26] G. Gokhroo,[44]
B. Golob,[21, 15] M. Grosse Perdekamp,[38] H. Guler,[9] J. Haba,[10] F. Handa,[47] K. Hara,[10]
T. Hara,[34] N. C. Hastings,[10] K. Hasuko,[38] K. Hayasaka,[24] H. Hayashii,[25] M. Hazumi,[10]
E. M. Heenan,[23] I. Higuchi,[47] T. Higuchi,[10] L. Hinz,[20] T. Hojo,[34] T. Hokuue,[24]
Y. Hoshi,[46] K. Hoshina,[51] S. Hou,[26] W.-S. Hou,[29] Y. B. Hsiung,[29] H.-C. Huang,[29]
T. Igaki,[24] Y. Igarashi,[10] T. Iijima,[24] A. Imoto,[25] K. Inami,[24] A. Ishikawa,[10] H. Ishino,[49]
K. Itoh,[48] R. Itoh,[10] M. Iwamoto,[3] M. Iwasaki,[48] Y. Iwasaki,[10] R. Kagan,[14] H. Kakuno,[48]
J. H. Kang,[56] J. S. Kang,[17] P. Kapusta,[30] S. U. Kataoka,[25] N. Katayama,[10] H. Kawai,[3]
H. Kawai,[48] Y. Kawakami,[24] N. Kawamura,[1] T. Kawasaki,[32] N. Kent,[9] H. R. Khan,[49]
A. Kibayashi,[49] H. Kichimi,[10] H. J. Kim,[19] H. O. Kim,[42] Hyunwoo Kim,[17] J. H. Kim,[42]
S. K. Kim,[41] T. H. Kim,[56] K. Kinoshita,[6] P. Koppenburg,[10] S. Korpar,[22, 15] P. Križan,[21, 15]
P. Krokovny,[2] R. Kulasiri,[6] C. C. Kuo,[26] H. Kurashiro,[49] E. Kurihara,[3] A. Kusaka,[48]
A. Kuzmin,[2] Y.-J. Kwon,[56] J. S. Lange,[7] G. Leder,[13] S. E. Lee,[41] S. H. Lee,[41]
Y.-J. Lee,[29] T. Lesiak,[30] J. Li,[40] A. Limosani,[23] S.-W. Lin,[29] D. Liventsev,[14]
J. MacNaughton,[13] G. Majumder,[44] F. Mandl,[13] D. Marlow,[37] T. Matsuishi,[24]
H. Matsumoto,[32] S. Matsumoto,[5] T. Matsumoto,[50] A. Matyja,[30] Y. Mikami,[47]
W. Mitaroff,[13] K. Miyabayashi,[25] Y. Miyabayashi,[24] H. Miyake,[34] H. Miyata,[32] R. Mizuk,[14]
D. Mohapatra,[55] G. R. Moloney,[23] G. F. Moorhead,[23] T. Mori,[49] A. Murakami,[39]
T. Nagamine,[47] Y. Nagasaka,[11] T. Nakadaira,[48] I. Nakamura,[10] E. Nakano,[33] M. Nakao,[10]
H. Nakazawa,[10] Z. Natkaniec,[30] K. Neichi,[46] S. Nishida,[10] O. Nitoh,[51] S. Noguchi,[25]
T. Nozaki,[10] A. Ogawa,[38] S. Ogawa,[45] T. Ohshima,[24] T. Okabe,[24] S. Okuno,[16]
S. L. Olsen,[9] Y. Onuki,[32] W. Ostrowicz,[30] H. Ozaki,[10] P. Pakhlov,[14] H. Palka,[30]
C. W. Park,[42] H. Park,[19] K. S. Park,[42] N. Parslow,[43] L. S. Peak,[43] M. Pernicka,[13]
J.-P. Perroud,[20] M. Peters,[9] L. E. Piilonen,[55] A. Poluektov,[2] F. J. Ronga,[10] N. Root,[2]
M. Rozanska,[30] H. Sagawa,[10] M. Saigo,[47] S. Saitoh,[10] Y. Sakai,[10] H. Sakamoto,[18]
T. R. Sarangi,[10] M. Satapathy,[54] N. Sato,[24] O. Schneider,[20] J. Schümann,[29] C. Schwanda,[13]
A. J. Schwartz,[6] T. Seki,[50] S. Semenov,[14] K. Senyo,[24] Y. Settai,[5] R. Seuster,[9]
M. E. Sevior,[23] T. Shibata,[32] H. Shibuya,[45] B. Shwartz,[2] V. Sidorov,[2] V. Siegle,[38]
J. B. Singh,[35] A. Somov,[6] N. Soni,[35] R. Stamen,[10] S. Stanič,[53, *] M. Starič,[15] A. Sugi,[24]
A. Sugiyama,[39] K. Sumisawa,[34] T. Sumiyoshi,[50] S. Suzuki,[39] S. Y. Suzuki,[10] O. Tajima,[10]
F. Takasaki,[10] K. Tamai,[10] N. Tamura,[32] K. Tanabe,[48] M. Tanaka,[10] G. N. Taylor,[23]
Y. Teramoto,[33] X. C. Tian,[36] S. Tokuda,[24] S. N. Tovey,[23] K. Trabelsi,[9] T. Tsuboyama,[10]

T. Tsukamoto,[10] K. Uchida,[9] S. Uehara,[10] T. Uglov,[14] K. Ueno,[29] Y. Unno,[3] S. Uno,[10]
Y. Ushiroda,[10] G. Varner,[9] K. E. Varvell,[43] S. Villa,[20] C. C. Wang,[29] C. H. Wang,[28]
J. G. Wang,[55] M.-Z. Wang,[29] M. Watanabe,[32] Y. Watanabe,[49] L. Widhalm,[13]
Q. L. Xie,[12] B. D. Yabsley,[55] A. Yamaguchi,[47] H. Yamamoto,[47] S. Yamamoto,[50]
T. Yamanaka,[34] Y. Yamashita,[31] M. Yamauchi,[10] Heyoung Yang,[41] P. Yeh,[29] J. Ying,[36]
K. Yoshida,[24] Y. Yuan,[12] Y. Yusa,[47] H. Yuta,[1] S. L. Zang,[12] C. C. Zhang,[12] J. Zhang,[10]
L. M. Zhang,[40] Z. P. Zhang,[40] V. Zhilich,[2] T. Ziegler,[37] D. Žontar,[21, 15] and D. Zürcher[20]

(The Belle Collaboration)

[1]*Aomori University, Aomori*
[2]*Budker Institute of Nuclear Physics, Novosibirsk*
[3]*Chiba University, Chiba*
[4]*Chonnam National University, Kwangju*
[5]*Chuo University, Tokyo*
[6]*University of Cincinnati, Cincinnati, Ohio 45221*
[7]*University of Frankfurt, Frankfurt*
[8]*Gyeongsang National University, Chinju*
[9]*University of Hawaii, Honolulu, Hawaii 96822*
[10]*High Energy Accelerator Research Organization (KEK), Tsukuba*
[11]*Hiroshima Institute of Technology, Hiroshima*
[12]*Institute of High Energy Physics,*
Chinese Academy of Sciences, Beijing
[13]*Institute of High Energy Physics, Vienna*
[14]*Institute for Theoretical and Experimental Physics, Moscow*
[15]*J. Stefan Institute, Ljubljana*
[16]*Kanagawa University, Yokohama*
[17]*Korea University, Seoul*
[18]*Kyoto University, Kyoto*
[19]*Kyungpook National University, Taegu*
[20]*Swiss Federal Institute of Technology of Lausanne, EPFL, Lausanne*
[21]*University of Ljubljana, Ljubljana*
[22]*University of Maribor, Maribor*
[23]*University of Melbourne, Victoria*
[24]*Nagoya University, Nagoya*
[25]*Nara Women's University, Nara*
[26]*National Central University, Chung-li*
[27]*National Kaohsiung Normal University, Kaohsiung*
[28]*National United University, Miao Li*
[29]*Department of Physics, National Taiwan University, Taipei*
[30]*H. Niewodniczanski Institute of Nuclear Physics, Krakow*
[31]*Nihon Dental College, Niigata*
[32]*Niigata University, Niigata*
[33]*Osaka City University, Osaka*
[34]*Osaka University, Osaka*
[35]*Panjab University, Chandigarh*
[36]*Peking University, Beijing*
[37]*Princeton University, Princeton, New Jersey 08545*

[38]*RIKEN BNL Research Center, Upton, New York 11973*
[39]*Saga University, Saga*
[40]*University of Science and Technology of China, Hefei*
[41]*Seoul National University, Seoul*
[42]*Sungkyunkwan University, Suwon*
[43]*University of Sydney, Sydney NSW*
[44]*Tata Institute of Fundamental Research, Bombay*
[45]*Toho University, Funabashi*
[46]*Tohoku Gakuin University, Tagajo*
[47]*Tohoku University, Sendai*
[48]*Department of Physics, University of Tokyo, Tokyo*
[49]*Tokyo Institute of Technology, Tokyo*
[50]*Tokyo Metropolitan University, Tokyo*
[51]*Tokyo University of Agriculture and Technology, Tokyo*
[52]*Toyama National College of Maritime Technology, Toyama*
[53]*University of Tsukuba, Tsukuba*
[54]*Utkal University, Bhubaneswer*
[55]*Virginia Polytechnic Institute and State University, Blacksburg, Virginia 24061*
[56]*Yonsei University, Seoul*

Abstract

We report a study of the suppressed decay $B^- \to [K^+\pi^-]_D K^-$ (and its charge-conjugate mode) at Belle, where $[K^+\pi^-]_D$ indicates that the $K^+\pi^-$ pair originates from a neutral D meson. A data sample containing 274 million $B\bar{B}$ pairs recorded at the $\Upsilon(4S)$ resonance with the Belle detector at the KEKB asymmetric e^+e^- storage ring is used. This decay mode can be used to extract the CKM angle ϕ_3 using the so-called Atwood-Dunietz-Soni method. The signal for $B^- \to [K^+\pi^-]_D K^-$ has 2.7σ statistical significance, and we set a limit on the ratio of B decay amplitudes $r_B < 0.28$ at the 90% confidence level. We observe a signal with 5.8σ statistical significance in the related mode, $B^- \to [K^+\pi^-]_D \pi^-$.

PACS numbers:

INTRODUCTION

The extraction of ϕ_3, an angle in the Kobayashi-Maskawa triangle[1], is a challenging measurement even with modern high luminosity B factories. Several methods for measuring ϕ_3 use the interference between $B^- \to D^0 K^-$ and $B^- \to \bar{D}^0 K^-$, which occurs when D^0 and $\bar{D}^0$ decay to common final states[2]. In this paper, we analyze the suppressed decay $B^- \to [K^+\pi^-]_D K^-$ and its charge conjugate mode, where $[K^+\pi^-]_D$ indicates that the $K^+\pi^-$ pair originates from a neutral D meson. In this case, the color-allowed B decay followed by the doubly Cabbibo-suppressed D decay interferes with the color-suppressed B decay followed by the Cabbibo-allowed D decay(Fig.1). This decay mode can be used to extract ϕ_3 using the so-called Atwood-Dunietz-Soni method(ADS method)[3].
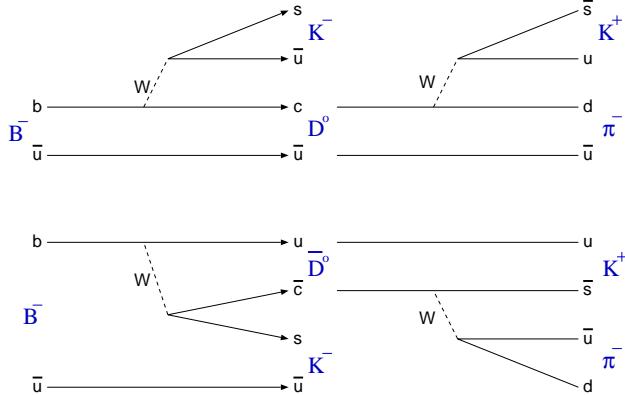
FIG. 1: $B^- \to [K^+\pi^-]_D K^-$ decays.

ADS METHOD

Here we define the amplitudes for B decays and D decays as follows:

$$A_B \equiv A(B^- \to D^0 K^-) = A(B^+ \to \bar{D}^0 K^+), \quad A_D \equiv A(D^0 \to \bar{f}) = A(\bar{D}^0 \to f),$$
$$\bar{A}_B \equiv A(B^- \to \bar{D}^0 K^-) = A(B^+ \to D^0 K^+), \quad \bar{A}_D \equiv A(D^0 \to f) = A(\bar{D}^0 \to \bar{f}).$$

The branching fractions for $B^\pm \to [f]_D K^\pm$ decays with D^0 and $\bar{D}^0$ decays to common final states f are given as follows:

$$\Gamma(B^- \to [f]_D K^-) = [r_B^2 + r_D^2 + 2r_B r_D \cos(-\phi_3 + \delta)]|A_B|^2|A_D|^2$$
$$\Gamma(B^+ \to [\bar{f}]_D K^+) = [r_B^2 + r_D^2 + 2r_B r_D \cos(\phi_3 + \delta)]|A_B|^2|A_D|^2,$$

where

$$r_B \equiv \left|\frac{\bar{A}_B}{A_B}\right|, \quad r_D \equiv \left|\frac{\bar{A}_D}{A_D}\right|, \quad \delta \equiv \delta_B + \delta_D$$

and δ_B and δ_D are the strong phase differences between the two B and D decays, respectively. The modulus of the amplitude, $|A_B|^2$ can be measured using a flavor specific D^0 decay mode.

If we use a D decay mode in which A_D and r_D are known, the above 2 equations have 3 unknowns(ϕ_3, r_B, δ). However, using two final states f_1 and f_2, there are 4 equations and 4 unknowns(ϕ_3, r_B, δ_1, δ_2), which can be solved for ϕ_3. Using multiple decay modes for $D \to f_i$, the value of ϕ_3, and other unknowns, can be extracted from a fit. The suppressed decay $B^- \to [K^+\pi^-]_D K^-$ is an especially useful mode for the ADS method. The two interfering amplitudes in this decay mode are comparable, and large CP violating asymmetries can be expected. This decay mode is thus sensitive to the value of ϕ_3.

ANALYSIS

In this paper, we report an analysis of the suppressed decay $B^\pm \to [K^\mp\pi^\pm]_D K^\pm$. We also analyzed the suppressed decay $B^\pm \to [K^\mp\pi^\pm]_D \pi^\pm$. In addition, the allowed decays $B^\pm \to [K^\pm\pi^\mp]_D K^\pm$ and $B^\pm \to [K^\pm\pi^\mp]_D \pi^-$ are used as control samples to reduce systematic uncertainties. The same selection criteria for the suppressed decay modes are applied to the control samples whenever possible. Throughout this report, charge conjugate states are implied except where explicitly mentioned and we denote the analyzed decay modes as follows.

$$\text{Suppressed decay } B^- \to [K^+\pi^-]_D h^- : \quad B^- \to D_{cs}h^-$$
$$\text{Allowed decay } \quad B^- \to [K^-\pi^+]_D h^- : \quad B^- \to D_f h^- (h = K, \pi)$$

The results are based on a data sample containing 274 million $B\bar{B}$ pairs, collected with the Belle detector at KEKB asymmetric energy e^+e^- collider operating at the $\Upsilon(4S)$ resonance. The Belle detector is a large-solid-angle magnetic spectrometer that consists of a silicon vertex detector (SVD), a 50-layer central drift chamber (CDC), an array of aerogel threshold Čerenkov counters (ACC), a barrel-like arrangement of time-of-flight scintillation counters (TOF), and an electromagnetic calorimeter (ECL) comprised of CsI(Tl) crystals located inside a super-conducting solenoid coil that provides a 1.5 T magnetic field. An iron flux-return located outside of the coil is instrumented to detect K_L^0 mesons and to identify muons (KLM). The detector is described in detail elsewhere [4]. Two different inner detector configurations were used. For the first sample of 152 million $B\bar{B}$ pairs, a 2.0 cm radius beampipe and a 3-layer silicon vertex detector were used; for the latter 122 million $B\bar{B}$ pairs, a 1.5 cm radius beampipe, a 4-layer silicon detector and a small-cell inner drift chamber were used[5].

Event selection

D mesons are reconstructed by combining two oppositely charged tracks. These charged tracks are required to have a point of closest approach to the beam line within ± 5 mm of the interaction point in the direction perpendicular to the beam axis(dr) and ± 5 cm in the direction parallel to the beam axis(dz). A K/π likelihood ratio $P(K/\pi) = \mathcal{L}_K/(\mathcal{L}_K + \mathcal{L}_\pi)$ is formed for each track, where $\mathcal{L}_K$ and $\mathcal{L}_\pi$ are kaon and pion likelihoods. We used the particle identification requirement $P(K/\pi) > 0.4$ and $P(K/\pi) < 0.7$ for kaons and pions from $D \to K\pi$ decays, respectively. D candidates are required to have an invariant mass within $\pm 2.5\sigma$ of the nominal D^0 mass: 1.850 GeV$/c^2 < M(K\pi) < 1.879$ GeV$/c^2$. To improve the momentum determination, tracks from the D candidate are refitted according to the nominal

D^0 mass hypothesis and the reconstructed vertex position (a mass-and-vertex-constrained fit).

B mesons are reconstructed by combining D candidates with primary charged hadron candidates. For the charged tracks, we require $P(K/\pi) > 0.6$ for the kaon in $B^- \to DK^-$ and $P(K/\pi) < 0.2$ for the pion in $B^- \to D\pi^-$. The signal is identified by two kinematic variables, the energy difference $\Delta E = E_D + E_{K^-(\pi^-)} - E_{\text{beam}}$ and the beam-energy-constrained mass $M_{\text{bc}} = \sqrt{E_{\text{beam}}^2 - (\vec{p}_D + \vec{p}_{K^-(\pi^-)})^2}$, where E_D is the energy of the D candidate, $E_{K^-(\pi^-)}$ is the energy of the $K^-(\pi^-)$ and E_{beam} is the beam energy, in the cm frame. $\vec{p}_D$ and $\vec{p}_{K^-(\pi^-)}$ are the momenta of the D and $K^-(\pi^-)$ in the cm frame. We define the signal region as $5.27 \text{ GeV}/c^2 < M_{\text{bc}} < 5.29 \text{ GeV}/c^2$ and $-0.04 \text{ GeV} < \Delta E < 0.04 \text{ GeV}$. In the case of multiple candidates per event, we choose the best candidate on the basis of a χ^2 determined from the difference between the measured and nominal values of M_D and M_{bc}.

$q\bar{q}$ continuum suppression

To suppressed the large background from the two-jet like $e^+e^- \to q\bar{q}(q = u, d, s, c)$ continuum processes, variables that characterize the event topology are used. We construct a Fisher discriminant of Fox-Wolfram moments called the Super-Fox-Wolfram(SFW) [6][7], where the Fisher coefficients are optimized by maximizing the separation between $B\bar{B}$ events and continuum events. Furthermore, $\cos\theta_B$, the angle in the cm system between the B flight direction with respect to the beam axis is used as another variable to distinguish $B\bar{B}$ events from continuum events. These two independent variables, SFW and $\cos\theta_B$ are combined to form a likelihood ratio(LR),

$$LR = \mathcal{L}_{\text{sig}}/(\mathcal{L}_{\text{sig}} + \mathcal{L}_{\text{cont}})$$
$$\mathcal{L}_{\text{sig(cont)}} = \mathcal{L}_{\text{sig(cont)}}^{SFW} \times \mathcal{L}_{\text{sig(cont)}}^{\cos\theta_B},$$

where $\mathcal{L}_{\text{sig}}$ and $\mathcal{L}_{\text{cont}}$ are likelihoods defined from SFW and $\cos\theta_B$ distributions for signal and continuum backgrounds, respectively. We optimized the LR requirement by maximizing a figure of merit, $S/\sqrt{S+N}$, where S and N denote the expected number of signal and background in the signal region. For $B^- \to D_{cs}K^-(\pi^-)$ we require $LR > 0.85(> 0.75)$, which retains 44.8%(57.6%) signal events and removes 96.2%(93.2%) of the continuum background.

Peaking backgrounds

For $B^- \to D_{cs}K^-$, one can have a contribution from $B^- \to D^0\pi^-$, $D^0 \to K^+K^-$, which has the same final state and can peak under the signal. In order to reject these events, we veto events that satisfy $1.843 \text{ GeV}/c^2 < M(KK) < 1.894 \text{ GeV}/c^2$. The allowed decay $B^- \to D_f h^-$ can also be a peaking background for the suppressed decay modes due to $K\pi$ misidentification. Therefore, we veto events for which the invariant mass of the $K\pi$ pair is inside the D mass cut window when the mass assignments are exchanged. Furthermore, three-body charmless decays $B^- \to K^+K^-\pi^-$ and $B^- \to K^+\pi^-\pi^-$ can peak inside the signal region for $B^- \to D_{cs}K^-$ and $B^- \to D_{cs}\pi^-$, respectively. These peaking backgrounds are estimated from the ΔE distributions of events in a D mass sideband, defined as $1.808 \text{ GeV}/c^2 < M(K\pi) < 1.836 \text{ GeV}/c^2$ and $1.893 \text{ GeV}/c^2 < M(K\pi) < 1.922 \text{ GeV}/c^2$, which

are shown in Fig.2. For $B^- \to D_{cs}\pi^-$, the peaking background estimated by fitting the plot is consistent with zero. Since the Standard Model prediction for the $B^- \to K^+\pi^-\pi^-$ branching fraction is smaller than 10^{-11}[8], this background contribution is ignored. On the other hand, for $B^- \to D_{cs}K^-$, the estimated peaking background is 3.1 ± 2.9 events inside the ΔE signal region after scaling to the D mass signal region. As a check, we naively estimate the expected background from the measured $B^- \to K^+K^-\pi^-$ mode. According to [9], the $B^- \to K^+K^-\pi^-$ yield is 94 ± 23 events with an efficiency of 13.8% (78.7 fb^{-1}). Using this result, the estimated background is

$$94 \times \frac{257.1 \text{ fb}^{-1}}{78.7 \text{ fb}^{-1}} \times \frac{\text{area}_D}{\text{area}_{Dalitz}} \times \frac{\text{eff}_{DK}}{\text{eff}_{KK\pi}} \sim 2.9 \text{ events},$$

where we assumed that the $B^- \to K^+K^-\pi^-$ yield is uniformly distributed over the Dalitz plot, and $\text{area}_D/\text{area}_{Dalitz}$ is the ratio between the D mass cut area and the Dalitz plot area, and $\text{eff}_{DK}/\text{eff}_{KK\pi}(= 17.5/13.8)$ is the ratio of the $B^- \to D_{cs}K^-$ efficiency to the $B^- \to K^+K^-\pi^-$ efficiency. This naive estimate is consistent with the estimate from the D^0 mass sideband. Therefore, we subtract 3.1 ± 2.9 events from the observed $B^- \to D_{cs}K^-$ yield.

After applying all the cuts, the signal efficiencies are 17.5% and 24.6% for $B^- \to D_{cs}K^-$ and $B^- \to D_{cs}\pi^-$, respectively. The signal yields are extracted by fitting the ΔE distributions.

Fitting the ΔE distributions

Backgrounds from decays such as $B^- \to D\rho^-$ and $B^- \to D^*\pi^-$ are distributed in the negative ΔE region and make a small contribution to the signal region. The shape of this $B\bar{B}$ background is modeled as a smoothed histogram from generic Monte Carlo (MC) samples. The continuum background populates the entire ΔE region. The shape of the continuum background is modeled as a linear function. The slope is determined from the ΔE distribution of the M_{bc} sideband data (5.20 GeV/$c^2 < M_{bc} < 5.26$ GeV/c^2).

The ΔE fitting function is the sum of two Gaussians for the signal, the linear function for the continuum, and the smoothed histogram for the $B\bar{B}$ background distribution.

In the fit to the ΔE distribution of $B^- \to D_f\pi^-$, the free parameters are the position, width and area of the signal peak, and the normalizations of continuum and $B\bar{B}$ backgrounds. The ratio of the two Gaussians of the signal is fixed from the signal MC. For the $B^- \to D_f K^-$ fit, the position and width of the signal peak are fixed from the $B^- \to D_f\pi^-$ fit results. To fit the feed-across from $D_f\pi^-$, we use a Gaussian shape where the left and right sides of the peak have different widths since the shift caused by wrong mass assignment makes the shape asymmetric. The shape parameters of this function are fixed at values determined by the fit to the $B^- \to D_f\pi^-$ distribution using a kaon mass hypothesis for the prompt pion. The areas of signal and feed-across from $D\pi^-$, and the normalizations of continuum and $B\bar{B}$ backgrounds are floated in the fit. For $B^- \to D_{cs}K^-$ and $B^- \to D_{cs}\pi^-$, the signal and $B\bar{B}$ background shapes are modeled using the fit results of the $B^- \to D_f K^-$ and $B^- \to D_f\pi^-$ modes, respectively. The area of the feed-across from $D_{cs}\pi^-$ is estimated as the measured yield of $B^- \to D_{cs}\pi^-$ multiplied by the π to K misidentification probability. However, the areas of the signal and the normalizations of continuum and $B\bar{B}$ backgrounds are floated. The fit results are shown in Fig.3. The numbers of events for $B^- \to D_{cs}h^-$

and $D_f h^-$, and the statistical significances of the $B^- \to D_{cs}h^-$ signals are given in Table I. The statistical significance is defined as $\sqrt{-2\ln(\mathcal{L}_0/\mathcal{L}_{\max})}$, where $\mathcal{L}_{\max}$ is the maximum likelihood in the ΔE fit and $\mathcal{L}_0$ is the likelihood when the signal yield is constrained to be zero. The uncertainty in the peaking background contribution is taken into account in the statistical significance calculation. The statistical significance of the $B^- \to D_{cs}\pi^-$ signal is over 5.0σ.

TABLE I: Signal yields and efficiency. For the $B^- \to D_{cs}K^-$ signal yield, the peaking background contribution has been subtracted.

Mode	Product branching fraction from PDG	Efficiency (%)	Signal Yield	Statistical significance
$B^- \to D_{cs}K^-$	$-$	17.5 ± 0.2	$14.7^{+8.0}_{-7.3}$	2.7
$B^- \to D_{cs}\pi^-$	$(6.9 \pm 0.7) \times 10^{-7}$	24.6 ± 0.2	$30.7^{+9.1}_{-8.4}$	5.8
$B^- \to D_f K^-$	$(1.4 \pm 0.2) \times 10^{-5}$	17.5 ± 0.3	$535.0^{+18.8}_{-18.2}$	
$B^- \to D_f \pi^-$	$(1.9 \pm 0.1) \times 10^{-4}$	24.7 ± 0.2	10178^{+105}_{-104}	

RESULTS

Branching fraction of suppressed decay modes

The branching fractions for $B^- \to D_{cs}h^-(h = K, \pi)$ are determined as

$$\mathcal{B}(B^- \to D_{cs}h^-) = \mathcal{B}(B^- \to D_f h^-) \times \frac{N_{D_{cs}h}}{N_{D_f h}},$$

where $N_{D_{cs}h}$ and $N_{D_f h}$ are the number of $B^- \to D_{cs}h^-$ signal events and $B^- \to D_f h^-$ signal events. The product branching fractions for $B^- \to D_f h^-$, calculated from the world averages for the branching fractions [10], are given in Table I. Using these, the branching fractions for the suppressed decays $B^- \to D_{cs}h^-$ are found to be

$$\mathcal{B}(B^- \to [K^+\pi^-]_D K^-) = (3.9^{+2.1}_{-1.9}(stat) \pm 0.2(sys) \pm 0.6(PDG)) \times 10^{-7},$$
$$\mathcal{B}(B^- \to [K^+\pi^-]_D \pi^-) = (5.7^{+1.7}_{-1.6}(stat) \pm 0.3(sys) \pm 0.3(PDG)) \times 10^{-7}.$$

Most of the systematic uncertainties from the detection efficiencies and the particle identification cancel when taking the ratios, since the kinematics of the $B^- \to D_{cs}h^-$ and $B^- \to D_f h^-$ processes are similar. The systematic errors are due to the uncertainty in the yield extraction and the efficiency difference between $B^- \to D_{cs}h^-$ and $B^- \to D_f h^-$. The uncertainties in the signal shapes and the $q\bar{q}$ background shapes are determined by varying the shape of the fitting function by $\pm 1\sigma$. The uncertainties in the $B\bar{B}$ background shapes are determined by fitting the ΔE distribution in the region -0.07 GeV $< \Delta E <$ 0.20 GeV ignoring the $B\bar{B}$ background contributions. The uncertainties in the efficiency differences are determined by the signal MC. The total systematic errors are obtained as the quadratic sum of those uncertainties. The results are shown in Table II.

8

The uncertainties in the branching fractions are statistics-dominated. For the $B^- \rightarrow D_{cs}K^-$ branching fraction, we set an upper limit at the 90% confidence level as

$$\mathcal{B}(B^- \rightarrow D_{cs}K^-) < 7.6 \times 10^{-7}(90\% \text{ C.L.}),$$

where we took the likelihood function as a single gaussian with width given by the quadratic sum of the statistical and systematic errors, and the area is normalized in the physical region of positive branching fraction.

TABLE II: Systematic uncertainties for $B^- \rightarrow DK^-$ and $B^- \rightarrow D\pi^-$.

Source	Systematic error(%)			
	$D_{cs}K^-$	D_fK^-	$D_{cs}\pi^-$	$D_f\pi^-$
$B\bar{B}$ background shape	± 2.1	± 1.0	± 4.6	± 1.6
$q\bar{q}$ background shape	± 3.6	± 0.4	± 1.9	± 0.1
Signal shape	± 0.6	± 0.4	± 1.4	± 0.2
Feed-across shape	± 1.4	± 1.0	$-$	$-$
Efficiency difference	± 1.5		± 1.3	
PDG Normalization	± 14.3		± 5.3	
Total	$\pm 4.9 \pm 14.3_{(PDG)}$		$\pm 5.5 \pm 5.3_{(PDG)}$	

Ratio of branching fractions R_{Dh}

We define the ratio

$$R_{Dh} \equiv \frac{\mathcal{B}(B^- \rightarrow D_{cs}h^-) + \mathcal{B}(B^+ \rightarrow D_{cs}h^+)}{\mathcal{B}(B^- \rightarrow D_f h^-) + \mathcal{B}(B^+ \rightarrow D_f h^+)} \quad (h = K, \pi)$$

$$= \frac{N_{D_{cs}h}}{N_{D_f h}}.$$

The ratios R_{Dh} are determined as follows

$$R_{DK} = (2.8^{+1.5}_{-1.4}(stat) \pm 0.1(sys)) \times 10^{-2},$$
$$R_{D\pi} = (3.0^{+0.9}_{-0.8}(stat) \pm 0.2(sys)) \times 10^{-3}$$

and

$$R_{DK} < 4.7 \times 10^{-2}(90\% \text{ C.L.}).$$

The ratio R_{DK} is related to ϕ_3 by

$$R_{DK} = r_B^2 + r_D^2 + 2r_B r_D \cos \phi_3 \cos \delta,$$

where

$$r_D = \left| \frac{A(D^0 \rightarrow K^+\pi^-)}{A(D^0 \rightarrow K^-\pi^+)} \right| = 0.060 \pm 0.003.$$

Using the above result, we obtain a limit on r_B. The least restrictive limit is obtained allowing $\pm 1\sigma$ variation on r_D [10] and assuming maximal interference($\phi_3 = 0°, \delta = 180°$ or $\phi_3 = 180°, \delta = 0°$) and is found to be

$$r_B < 0.28.$$

CP asymmetry

We search for partial rate asymmetries $\mathcal{A}_{Dh}$ in $B^\pm \to D_{cs}h^\pm$ decay, fitting the B^+ and B^- yields separately for each mode, where $\mathcal{A}_{Dh}$ is determined as

$$\mathcal{A}_{Dh} \equiv \frac{\mathcal{B}(B^- \to D_{cs}h^-) - \mathcal{B}(B^+ \to D_{cs}h^+)}{\mathcal{B}(B^- \to D_{cs}h^-) + \mathcal{B}(B^+ \to D_{cs}h^+)} \quad (h = K, \pi).$$

The peaking background for $B^- \to D_{cs}K^-$ is subtracted assuming no CP asymmetry. The fit results are shown in Fig.4 and Table III. We find

$$\mathcal{A}_{DK} = 0.49^{+0.53}_{-0.46}(stat) \pm 0.06(sys),$$
$$\mathcal{A}_{D\pi} = 0.12^{+0.30}_{-0.27}(stat) \pm 0.06(sys),$$

where the systematic uncertainty is from the intrinsic detector charge asymmetry, the B^+ and B^- yield extraction, and the asymmetry in particle identification efficiency of prompt kaons. The intrinsic detector charge asymmetry is determined from the $B^\pm \to D_f\pi^\pm$ samples. The systematic uncertainty from yield extraction is determined by varying the fitting parameters by $\pm 1\sigma$. The systematic uncertainty due to particle identification efficiency of prompt kaons is explained in [12]. The total systematic errors are combined as the quadratic sum of those uncertainties (Table IV). The measured partial rate asymmetries $\mathcal{A}_{Dh}$ are consistent with zero.

TABLE III: Signal yields and partial rate asymmetries.

Mode	$N(B^-)$	$N(B^+)$	$\mathcal{A}_{Dh}$
$B \to D_{cs}K$	$11.2^{+6.1}_{-5.4}$	$3.9^{+4.9}_{-4.3}$	$0.49^{+0.53}_{-0.46} \pm 0.06$
$B \to D_{cs}\pi$	$17.2^{+6.5}_{-5.8}$	$13.6^{+6.6}_{-5.9}$	$0.12^{+0.30}_{-0.27} \pm 0.06$

TABLE IV: Source of systematic uncertainties for the asymmetry calculation.

	Systematic error(%)	
Source	$\mathcal{A}_{DK}$	$\mathcal{A}_{D\pi}$
Yield extraction	4.8	4.9
Intrinsic detector charge asym	2.5	2.5
PID efficiency of prompt kaons	1.0	–
Total	5.5	5.5

SUMMARY

Using 274 million $B\bar{B}$ pairs collected with the Belle detector, we report studies of the suppressed decay $B^- \to D_{cs}h^-(h = K, \pi)$. We observe $B^- \to D_{cs}\pi^-$ for the first time, with a significance of 5.8σ. The size of the signal is consistent with expectation based on measured branching fractions [10]. The significance for $B^- \to D_{cs}K^-$ is 2.7σ and we set an upper limit on the ratio of B decay amplitudes r_B. This result is consistent with the measurement of r_B in the decay $B^- \to DK^-$, $D \to K_S\pi^+\pi^-$ [13].

Acknowledgments

   * on leave from Nova Gorica Polytechnic, Nova Gorica

[1] M. Kobayashi and T. Maskawa, Prog. Theor. Phys. **49**, 652 (1973).

[2] M. Gronau and D. Wyler, Phys. Lett. B **165**, 172 (1991); M. Gronau and D. London, Phys. Lett. B **253**, 483 (1991).

[3] D. Atwood, I. Dunietz, and A. Soni, Phys. Rev. Lett. **78**, 3257 (1997); Phys. Rev. D **63**, 036005 (2001)

[4] A. Abashian *et al.* (Belle collaboration), Nucl. Instr. and Meth. A **479**, 117 (2002).

[5] Y. Ushiroda (Belle SVD2 Group), Nucl. Instr. and Meth. A **511**, 6 (2003).

[6] R.A. Fisher, Ann. Eugenics **7**, 179 (1936).

[7] The Fox-Wolfram moments were introduce in G.C. Fox and S. Wolfram, Phys. Rev. Lett. **41**, 1581 (1978). The Fisher discriminant used by Belle, based on modified Fox-Wolfram moments(SFW), is described in K. Abe *et al.* (Belle collaboration), Phys. Rev. Lett. **87**, 101801 (2001) and K. Abe *et al.* (Belle collaboration), Phys. Lett. B **511**, 151 (2001).

[8] K. Huitu, C.D. Lu, P. Singer, D.X. Zhang, Phys. Rev. Lett. **81**, 4313 (1998).

[9] A.Garmash *et al.* (Belle collaboration), Phys. Rev. D **69**, 012001 (2004).

[10] S. Eidelman *et al.* (Particle Data Group), Phys. Lett. B **592**, 1 (2004).

[11] B. Aubert *et al.* (BaBar collaboration), hep-ex/0402024.

[12] S.K. Swain *et al.* (Belle collaboration), Phys. Rev. D **68**, 051101 (2003).

[13] A. Poluektov *et al.* (Belle collaboration), hep-ex/0406067 submitted to Phys. Rev. D.
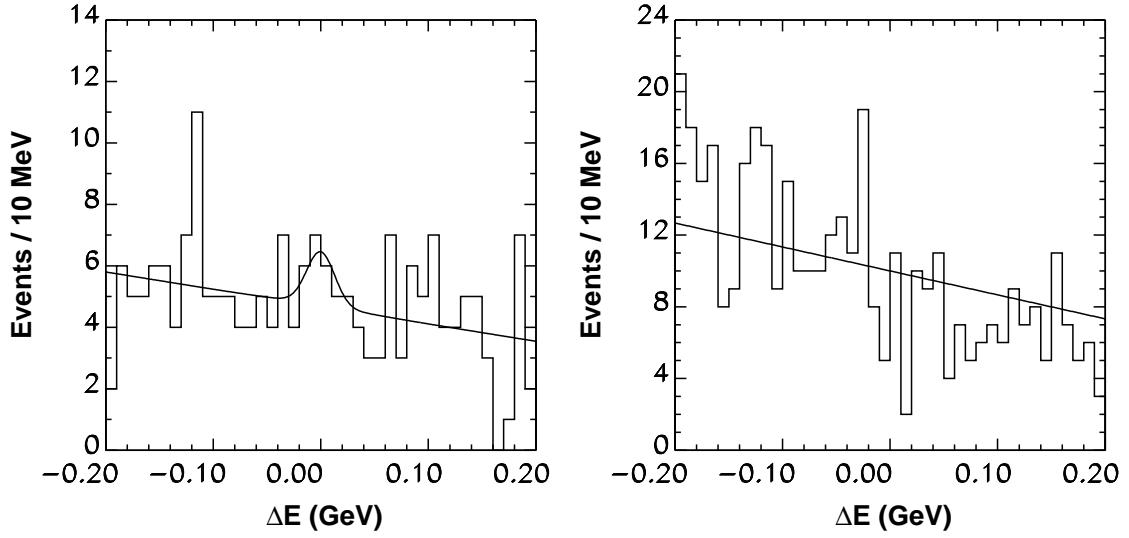
FIG. 2: ΔE distributions for events in the D^0 mass sideband for $B^- \to D_{cs}K^-$(left) and $B^- \to D_{cs}\pi^-$(right). The signal shapes are modeled using the results of the $B^- \to D_f h^- (h = K, \pi)$ fit.
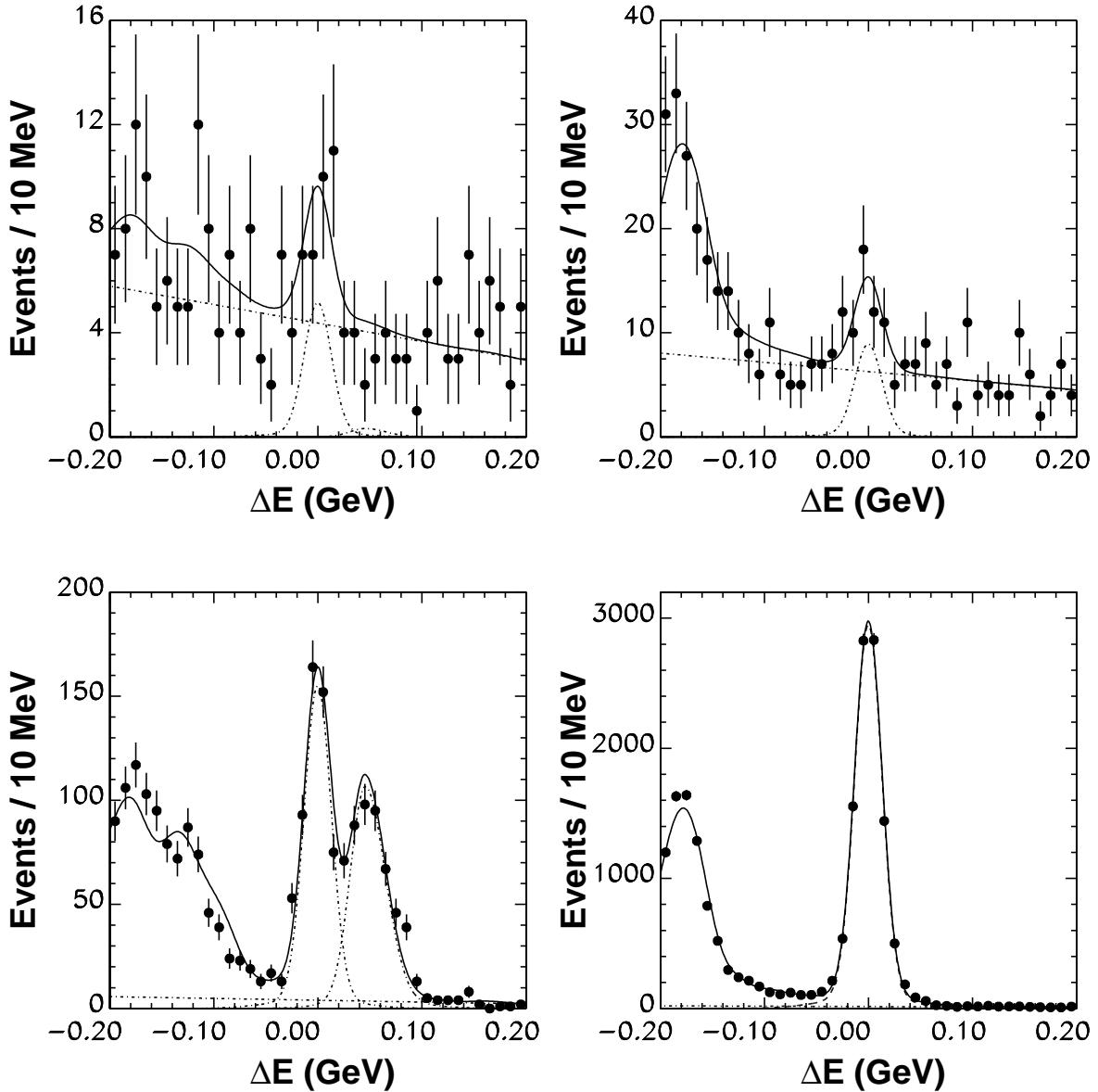
FIG. 3: ΔE fit results for $B^- \to D_{cs}K^-$(top-left), $B^- \to D_{cs}\pi^-$(top-right), $B^- \to D_f K^-$(bottom-left), and $B^- \to D_f \pi^-$(bottom-right). The charge conjugate modes are included for these plots.
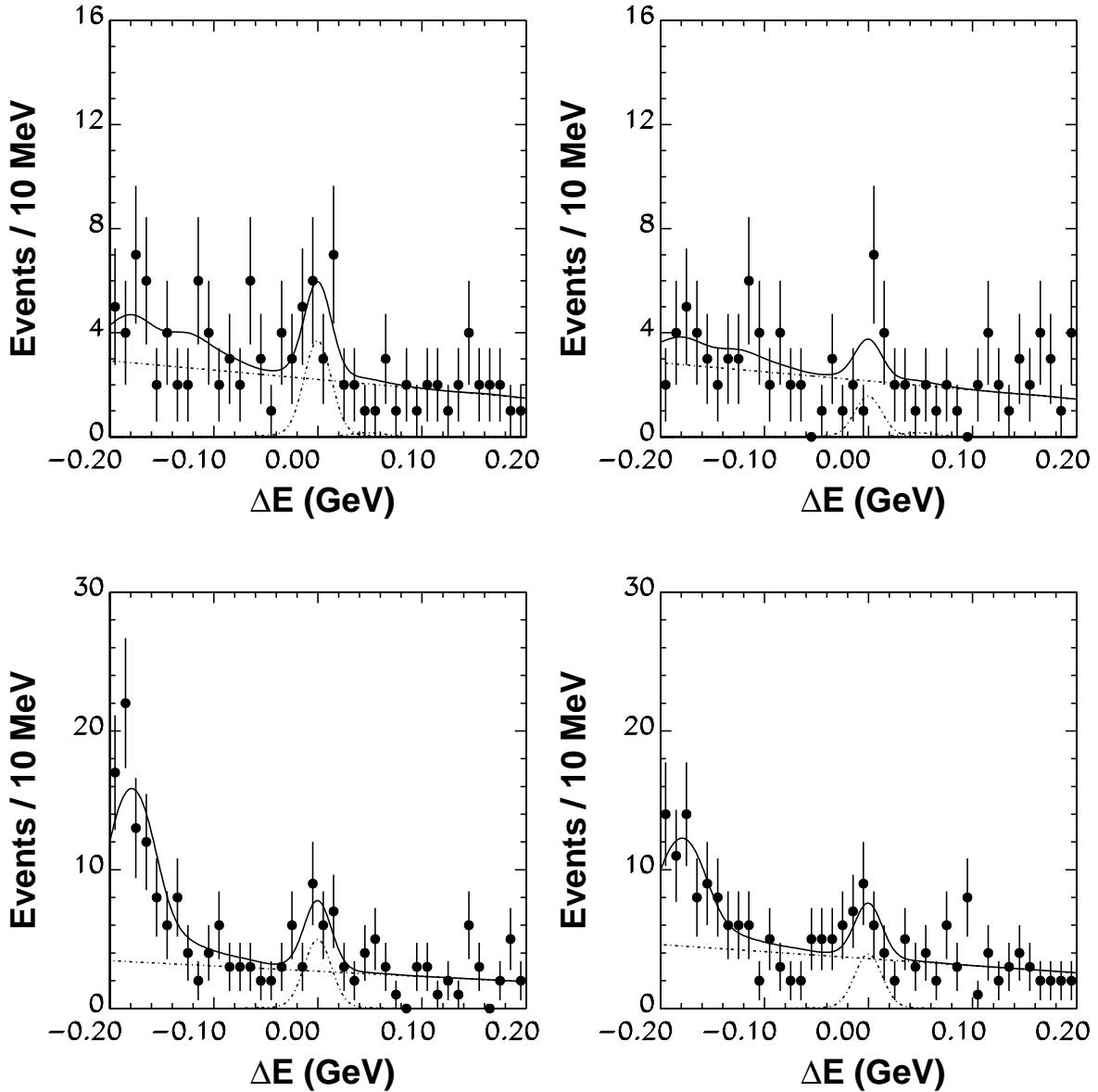
FIG. 4: ΔE fit results for $B^- \to D_{cs}K^-$(top-left), $B^+ \to D_{cs}K^+$(top-right), $B^- \to D_{cs}\pi^-$(bottom-left), and $B^+ \to D_{cs}\pi^+$(bottom-right).